

Constructing Compact ADAPT Unitary Coupled-Cluster Ansatz with Parameter-Based Criterion

Runhong He¹, Xin Hong¹, Qiaozhen Chai¹, Ji Guan¹, Junyuan Zhou², Arapat Ablimit³, Guolong Cui⁴ and Shenggang Ying^{1*}

1. *Key Laboratory of System Software (Chinese Academy of Sciences), Institute of Software, Chinese Academy of Sciences, Beijing 100190, China.*
2. *MindSpore Quantum Special Interest Group, China.*
3. *College of Physical Science and Technology, Xinjiang University, Urumqi 830017, China.*
4. *Arclight Quantum Computing Inc., Beijing 100086, China.*

The adaptive derivative-assembled pseudo-trotter variational quantum eigensolver (ADAPT-VQE) is a promising hybrid quantum-classical algorithm for molecular ground state energy calculation, yet its practical scalability is hampered by redundant excitation operators and excessive measurement costs. To address these challenges, we propose Param-ADAPT-VQE, a novel improved algorithm that selects excitation operators based on a parameter-based criterion instead of the traditional gradient-based metric. This strategy effectively eludes redundant operators. We further develop a sub-Hamiltonian technique and integrate a hot-start VQE optimization strategy, achieving a significant reduction in measurement costs. Numerical experiments on typical molecular systems demonstrate that Param-ADAPT-VQE outperforms the original ADAPT-VQE in computational accuracy, ansatz size, and measurement costs. Furthermore, our scheme retains the fundamental framework of ADAPT-VQE and is thus fully compatible with its various modified versions, enabling further performance improvements in specific aspects. This work presents an efficient and scalable enhancement to ADAPT-VQE, mitigating the core obstacles that impede its practical implementation in the field of molecular quantum chemistry.

I. INTRODUCTION

The accurate calculation of molecular energy levels lies at the heart of quantum chemistry [1], as it yields critical insights into chemical reactivity, material properties, and molecular dynamics [2]. However, classical computational approaches, such as the full configuration interaction (FCI), exhibit inherent limitations in addressing large molecular systems and strongly correlated systems, arising from the exponential scaling of computational complexity with increasing system size [3].

The emergence of quantum computing [4] offers a promising solution to this challenge, and the variational quantum eigensolver (VQE) algorithm [5–7] is among the most promising and widely investigated approaches for future quantum chemistry applications. VQE leverages the variational principle [8] to find the ground state energy of a target system by minimizing the expectation value of its Hamiltonian with respect to a parameterized quantum state (ansatz). The key advantage of VQE lies in that it splits the computational task between quantum and classical devices: the quantum processor prepares the ansatz and measures the Hamiltonian expectation value, while the classical optimizer adjusts the variational parameters iteratively. This hybrid quantum-classical architecture renders VQE compatible with near-

term noisy intermediate-scale quantum (NISQ) devices [9], which suffer from non-negligible gate errors, environmental noise, and a limited number of available qubits.

Despite its practicality, the performance of VQE is highly dependent on the design of the ansatz. A well-constructed ansatz should be expressive enough to approximate the ground state of the target system accurately while at the same time remaining shallow enough to be implementable on NISQ devices [3]. Traditional fixed ansatze (e.g., unitary coupled cluster singles and doubles, UCCSD [10–12]) often require a large number of excitation operators to achieve sufficient accuracy for complex molecular systems, thereby increasing noise susceptibility and exacerbating training challenges.

To address this limitation, the adaptive derivative-assembled pseudo-trotter (ADAPT) VQE [13] was developed as a problem-driven ansatz construction method. It builds the ansatz incrementally by selecting only the excitation operator with maximum initial gradient from a pre-defined operator pool in each iteration. Furthermore, ADAPT-VQE has been shown to mitigate optimization challenges associated with barren plateaus [14] and local minima [15]. ADAPT-VQE and its modified versions [16–25] have been widely applied to diverse molecular systems and have demonstrated superior performance in balancing ansatz expressivity and depth.

Nevertheless, ADAPT-VQE still faces two key challenges: (1) The gradient-based criterion is not infallible. Several studies [21, 23, 24] have noted that many excita-

* yingsg@ios.ac.cn

tion operators with the largest initial gradient are subsequently identified as redundant ones that fail to induce an effective energy reduction after optimization. They [21, 24] resort to an energy-based criterion, but incur a quartic additional measurement cost. (2) The compactness of the ADAPT-VQE ansatz comes at the cost of a surge in measurement overhead. While measurement cost is not the critical bottleneck at the current stage, excessively high measurement cost will still restrict the application to larger molecules [13, 26].

To address these challenges, we propose the Param-ADAPT-VQE algorithm with three core improvements: a novel parameter-based excitation operator selection criterion to reduce ansatz redundancy, a sub-Hamiltonian technique to suppress the measurement cost surge from operator pool scanning, and a hot-start training strategy to cut the measurement cost of global VQE optimization. Benchmark experiments on a variety of molecular systems demonstrate that, compared with ADAPT-VQE, Param-ADAPT-VQE exhibits superior performance in terms of the number of excitation operators, computational accuracy, and measurement cost.

The remainder of this paper is organized as follows: In Subsection II A, we introduce the fundamentals of the VQE and ADAPT-VQE algorithms. In Subsection II B, we elaborate on the proposed Param-ADAPT-VQE algorithm in detail. Numerical experiments are performed in Section III, and our conclusions are presented in Section IV. Additional performance comparisons for 6 typical molecules at varying bond lengths are provided in Appendix A for further reference.

II. METHODS

A. VQE and ADAPT-VQE

In the present work, indices i, j, k, \dots label occupied spin orbitals, while a, b, c, \dots denote virtual spin orbitals. Spin orbitals of both types are indexed by p, q, r, s . The total number of spin orbitals involved in a system of interest is denoted as N .

Under the Born-Oppenheimer approximation [1], where the molecular nuclei are treated as stationary, the second-quantized electronic Hamiltonian of a molecule in atomic units is given by the following form [3]:

$$\hat{H} = \sum_{p,q}^N h_q^p \hat{a}_p^\dagger \hat{a}_q + \frac{1}{2} \sum_{p,q,r,s}^N h_{rs}^{pq} \hat{a}_p^\dagger \hat{a}_q^\dagger \hat{a}_r \hat{a}_s, \quad (1)$$

where \hat{a}_i^\dagger and \hat{a}_i are the fermionic creation and annihilation operators, respectively. The electron integrals h_q^p and h_{rs}^{pq} can be computed classically within a specified basis set, such as the minimal STO-3G [1]. The fermionic Hamiltonian (1) can be mapped to Pauli strings via transformations such as the Jordan-Wigner [27], and its expectation value in a trial state $|\psi(\boldsymbol{\theta})\rangle$ can then be derived through measurement.

The trial state $|\psi(\boldsymbol{\theta})\rangle$ is prepared from a reference state $|\psi_{\text{ref}}\rangle$ via a moderately deep parameterized quantum circuit (ansatz) $U(\boldsymbol{\theta})$, such that $|\psi(\boldsymbol{\theta})\rangle = U(\boldsymbol{\theta})|\psi_{\text{ref}}\rangle$. The reference state $|\psi_{\text{ref}}\rangle$ is usually chosen as the Hartree-Fock state $|\text{HF}\rangle$. The measurement cost is proportional to the number of terms in the fermionic Hamiltonian (1), scaling as $O(N^4)$.

Within the VQE framework, an upper limit for the unknown ground-state energy E_0 can be derived by minimizing the Hamiltonian expectation value with respect to the variational parameters $\boldsymbol{\theta}$, according to the Rayleigh-Ritz variational principle [8]

$$\langle \psi(\boldsymbol{\theta}) | H | \psi(\boldsymbol{\theta}) \rangle \geq E_0. \quad (2)$$

The UCCSD is a commonly used chemistry-inspired ansatz which includes only single- and double-excitation operators to reduce the circuit depth, i.e.,

$$U(\boldsymbol{\theta}) = e^{\hat{T}(\boldsymbol{\theta})}, \quad (3)$$

where the anti-Hermitian operator

$$\hat{T}(\boldsymbol{\theta}) = \hat{T}_1(\boldsymbol{\theta}) + \hat{T}_2(\boldsymbol{\theta}), \quad (4)$$

$$\hat{T}_1(\boldsymbol{\theta}) = \sum_{i,a} \theta_i^a \hat{\tau}_i^a = \sum_{i,a} \theta_i^a \left(\hat{a}_a^\dagger \hat{a}_i - \hat{a}_i^\dagger \hat{a}_a \right), \quad (5)$$

$$\hat{T}_2(\boldsymbol{\theta}) = \sum_{a>b, i>j} \theta_{ij}^{ab} \hat{\tau}_{ij}^{ab} = \sum_{a>b, i>j} \theta_{ij}^{ab} \left(\hat{a}_a^\dagger \hat{a}_b^\dagger \hat{a}_i \hat{a}_j - \hat{a}_i^\dagger \hat{a}_j^\dagger \hat{a}_a \hat{a}_b \right). \quad (6)$$

Generally, the UCCSD ansatz contains $O\left(\binom{N/2}{1}^2\right) = O(N^2)$ single- and $O\left(\binom{N/2}{2}^2\right) = O(N^4)$ double-excitation operators, resulting in an overall $O(N^4)$ complexity [10, 12].

Within the first-order Trotter-Suzuki approximation [28], the above evolution operator can be decomposed as

$$e^{T(\boldsymbol{\theta})} \approx \prod_{i,a} e^{\hat{\tau}_i^a} \cdot \prod_{i>j, a>b} e^{\hat{\tau}_{ij}^{ab}}. \quad (7)$$

Since variational optimization can absorb the majority of truncation errors [29], this approximation is generally acceptable in VQE.

The circuit implementation of excitation operators has been extensively investigated in existing literature [20, 25, 30–32]. Among these studies, the method proposed in [33] has attracted widespread attention due to its remarkably shallow circuit depth, and we adopt this efficient circuit construction approach for all excitation operators in our work as well.

In contrast to the general-purpose and fixed ansatze, ADAPT-VQE constructs a problem-tailored ansatz on the fly. It defines an excitation operator pool (typically based on the UCCSD) and builds a compact quantum

circuit from the identity operator by appending only the excitation operator with the largest initial gradient magnitude from the pool at each iteration. Given that the measurement cost for computing the initial gradient of each operator is $O(N^3)$, for an operator pool with $O(N^4)$ size, the additional quantum measurements required to identify the proper excitation operator in each iteration scale as $O(N^7)$ [13]. Once the selected excitation operator is added to the ansatz, the algorithm executes a global VQE optimization on the updated ansatz with a warm start, i.e., the converged variational parameters from the preceding iteration act as the initial values for the current optimization and the parameter of the new operator is zero-initialized, enabling accelerated convergence by leveraging the pre-optimized solution [24]. This entire iterative cycle, consisting of excitation operator pool gradient evaluation, operator selection, and warm-started VQE optimization, is repeated until the pool's gradient norm drops below a pre-defined convergence threshold.

Theoretically, ADAPT-VQE can yield increasingly improved precision as iterative optimization progresses [13, 15]. However, several studies [21, 23, 24] have noted that ADAPT-VQE may incorporate numerous redundant operators in the ansatz, implying that the gradient-based selection criterion may not be optimal. Furthermore, the excessively high measurement cost also restricts its applicability to larger-scale problems. Next, we introduce our Param-ADAPT-VQE algorithm to mitigate these challenges.

B. Param-ADAPT-VQE

The general workflow of the Param-ADAPT-VQE algorithm is as follows:

Step 1. Define an excitation operator pool $\mathbb{P} := \{\hat{\tau}_q^p, \hat{\tau}_{rs}^{pq}\}$ and construct the full molecular fermionic Hamiltonian \hat{H} . For each excitation operator $\hat{\tau}_i \in \mathbb{P}$, extract the sub-Hamiltonian \hat{H}_i by selecting terms sharing indices with $\hat{\tau}_i$. Define iteration termination conditions: a parameter magnitude threshold $\epsilon > 0$ or a maximum iteration count $k_{\max} \geq 0$. Choose a suitable reference state $|\psi^{(0)}\rangle$ (e.g., the Hartree-Fock state $|\text{HF}\rangle$), initialize the ansatz as the identity operator $U \leftarrow U^{(0)} = \hat{I}$ and set the iteration index to $k = 1$.

Step 2. If $k > k_{\max}$, terminate the iterative procedure and proceed to Step 6; otherwise start the k^{th} iteration as follows: prepare the state $|\psi^{(k-1)}\rangle = U(\boldsymbol{\theta}^{(k-1)*})|\psi^{(0)}\rangle$, where $\boldsymbol{\theta}^{(k-1)*}$ denotes the optimized parameters from the $(k-1)^{\text{th}}$ iteration. We note that in this algorithm, the superscript $*$ denotes the optimized result, rather than the complex conjugate. For each excitation operator $\hat{\tau}_i \in \mathbb{P}$, perform a local VQE optimization to minimize the energy expectation value of the sub-Hamiltonian \hat{H}_i with respect to a new parameter θ_i until convergence, yielding the optimal parameter θ_i^* . The local VQE optimization

is defined as:

$$\theta_i^* = \underset{\theta_i}{\operatorname{argmin}} \langle \psi^{(k-1)*} | e^{\theta_i \hat{\tau}_i^\dagger} \hat{H}_i e^{\theta_i \hat{\tau}_i} | \psi^{(k-1)*} \rangle. \quad (8)$$

Step 3. If the maximum magnitude $|\theta_i^*| < \epsilon$, terminate the iterative procedure and proceed to Step 6.

Step 4. Select the excitation operator $\hat{\tau}_i$ with the maximum magnitude $|\theta_i^*|$, and append its corresponding unitary operator $e^{\theta_i^* \hat{\tau}_i}$ to the left of the current ansatz: $U(\boldsymbol{\theta}^{(k)}) \leftarrow e^{\theta_i^* \hat{\tau}_i} U(\boldsymbol{\theta}^{(k-1)*})$. Update the ansatz parameters set as $\boldsymbol{\theta}^{(k)} \leftarrow \boldsymbol{\theta}^{(k-1)*} \cup \{\theta_i^*\}$.

Step 5. Perform a global VQE optimization to re-optimize all variational parameters in the updated ansatz:

$$\boldsymbol{\theta}^{(k)*} = \underset{\boldsymbol{\theta}^{(k)}}{\operatorname{argmin}} \langle \psi^{(0)} | U^\dagger(\boldsymbol{\theta}^{(k)}) \hat{H} U(\boldsymbol{\theta}^{(k)}) | \psi^{(0)} \rangle. \quad (9)$$

Increment the iteration index as $k \leftarrow k + 1$ and return to Step 2.

Step 6. Evaluate the full Hamiltonian expectation value of the final trial state $|\psi^{(k)}\rangle = U(\boldsymbol{\theta}^{(k)*})|\psi^{(0)}\rangle$, i.e., $\langle \psi^{(k)} | \hat{H} | \psi^{(k)} \rangle$, and output this value as the molecular ground-state energy estimate.

We now provide some more detailed comments on the steps of the above Param-ADAPT-VQE protocol.

As described in Step 2, in a new iteration, Param-ADAPT-VQE tests each potential excitation operator $\hat{\tau}_i$ in the pool individually for the current trial state by assigning it a parameter θ_i and optimizing θ_i to convergence (i.e., local VQE optimization) to obtain the optimized θ_i^* ; the operator with the largest parameter magnitude $|\theta_i^*|$ is then selected and added to the ansatz. We note that, although this strategy involves more additional optimization steps than the gradient-based ADAPT-VQE, it does not actually incur a significant increase in experimental cost — and may even reduce it.

An important observation in fermionic semantics is that when individually optimizing the parameter of a new operator $\hat{\tau}_i$ in the ansatz, we only need to calculate this parameter's gradient and do not have to study the energy of the full hamiltonian \hat{H} . Here, “full” underscores that the Hamiltonian includes all non-zero excitation terms, rendering a size of $O(N^4)$ [3]. In this case, only those terms in \hat{H} that share indices with $\hat{\tau}_i$ contribute, i.e., $\{p, q, r, s\} \cap \{a, b, i, j\} \neq \emptyset$. Here, these two sets denote the indices of the Hamiltonian term and $\hat{\tau}_i$, respectively. Thus, we only need to collect these relevant terms from \hat{H} to form a new sub-Hamiltonian \hat{H}_i for computing the gradient of $\hat{\tau}_i$. For a single excitation operator, the size of the sub-Hamiltonian \hat{H}_i scales as $O\left(\binom{N}{1}^2 + \binom{N}{1}^4 - \binom{N-2}{1}^2 - \binom{N-2}{1}^4\right) = O(N^3)$. Similarly, for a double excitation operator, this count also scales as $O\left(\binom{N}{1}^2 + \binom{N}{1}^4 - \binom{N-4}{1}^2 - \binom{N-4}{1}^4\right) = O(N^3)$.

Employing the parameter-shift rule [34, 35], the gradient of a variational parameter can be calculated by the

discrepancy in interested Hamiltonian expectation values between several quantum circuits with shifted parameters. Using the Broyden-Fletcher-Goldfarb-Shanno (BFGS) minimizer [36], optimizing an ansatz $U(\theta^{(m)})$ with m variational parameters generally requires $O(m^2)$ VQE gradient evaluations [24]. Since only one variational parameter is involved in local VQE optimization, the number of gradient evaluations required for convergence is $O(1)$. Given that the size of the sub-Hamiltonian is $O(N^3)$, the total measurement cost for obtaining the converged parameter values of all excitation operators in the pool (with a size of $O\left(\binom{N}{2} + \binom{N}{4}\right) = O(N^4)$) is $O(N^7)$, which matches the selection cost of gradient-based ADAPT-VQE. However, by adopting the optimized new parameter values, the starting point for the global VQE optimization in Step 5 can be positioned closer to the optimal solution compared to the warm-start strategy used in ADAPT-VQE, which initiates global VQE optimization with the new parameter set to 0. We term this approach “hot-start”. This may significantly reduce the number of global optimization iterations and thus lower the total measurement cost. For strongly correlated molecules with larger sizes, the ansatz typically contains more excitation operators and variational parameters. Hot-start may introduce more pronounced benefits compared to warm-start in these cases. This claim is demonstrated by the numerical experiments in the next section.

The iteration termination condition for Param-ADAPT-VQE is that the parameter magnitude $|\theta_i^*|$ of the new operator falls below a threshold $\epsilon > 0$, or that the number of iterations exceeds a limit $k_{\max} > 0$.

We note that compared to ADAPT-VQE, Param-ADAPT-VQE modifies the criterion for selecting excitation operators while retaining its fundamental framework. It is therefore equally compatible with numerous derivative variants and inherits their respective advantages — such as adding multiple parallel excitation operators at once to reduce circuit depth [16], adopting advanced schemes for excitation operator implementation [24, 32], and removing redundant operators that already exist in ansatz [23].

III. NUMERICAL RESULTS

In this section, we present comprehensive numerical experiments to validate the performance of the proposed Param-ADAPT-VQE algorithm against the standard ADAPT-VQE. The analysis is divided into two dedicated subsections with hierarchical research objectives: Subsection III A focuses on a fine-grained, in-depth performance comparison using the BeH_2 molecule as a prototype system, demonstrating that the gradient-based selection criterion in ADAPT-VQE is not infallible and that the parameter constitutes a more robust criterion for avoiding redundant operators. Subsection III B further

conducts systematic benchmark studies on three additional molecular systems (LiH , H_2O and NH_3), with a focus on three key practical metrics — energy error, parameter count, and measurement cost — to verify the scalability and effectiveness of Param-ADAPT-VQE across diverse molecular systems. Collectively, these results provide both microscopic mechanistic insights and macroscopic practical validation for the proposed algorithm’s improvements over the ADAPT-VQE.

In this work, electronic integrals and molecular point groups are computed using PySCF [37], whereas second quantization, Jordan-Wigner transformation, and quantum circuit simulations are carried out via MindSpore Quantum [38]. Excitation operators are implemented based on the scheme [24, 33]. All computational procedures adopt the STO-3G basis set with no frozen orbitals considered, and the BFGS algorithm [36] integrated within the SciPy Python library [39] is applied to all optimization processes. The excitation operator pool is constructed based on the Hamiltonian-Informed UCCSD ansatz [12], which leverages information inherent in the molecular Hamiltonian to drastically reduce the number of excitation operators compared to UCCSD, without compromising its expressibility. All simulations in this work are performed under idealized scenarios that exclude both sampling noise and hardware-related noise.

A. Detailed Performance Analysis on BeH_2 molecule

To ground this discussion in concrete context, we take the ground-state simulation of the BeH_2 molecule with two symmetrically stretched bonds and $\text{R}(\text{Be-H})=2.6\text{\AA}$ as a paradigmatic example. Strongly correlated systems such as this are notably challenging, typically requiring long ansatze to reach sufficient computational accuracy. We note that while chemical accuracy (1.6 mHartree) is defined in the complete basis set limit or relative to experimental results, rather than the STO-3G basis set adopted in this work, it is nonetheless marked in the figures as a convention to facilitate readers in making comparisons with results from other related studies [11, 13, 23, 24]. In the discussion, we sometimes impose more stringent accuracy requirements, such as 10^{-4} and 10^{-5} Hartree. Furthermore, we emphasize that both Param-ADAPT-VQE and ADAPT-VQE can achieve higher accuracy by setting more stringent stopping conditions. In this section, the norm thresholds for Param-ADAPT-VQE and ADAPT-VQE are set to 10^{-4} and 10^{-3} , respectively, and the maximum number of iterations is fixed at 120.

Figure 1(a) depicts the evolution of energy error relative to the FCI result for ADAPT-VQE and Param-ADAPT-VQE as a function of iteration number. It can be observed that to reach a comparable error level of 10^{-4} Hartree, ADAPT-VQE requires 54 excitation operators, whereas Param-ADAPT-VQE only uses 39, representing

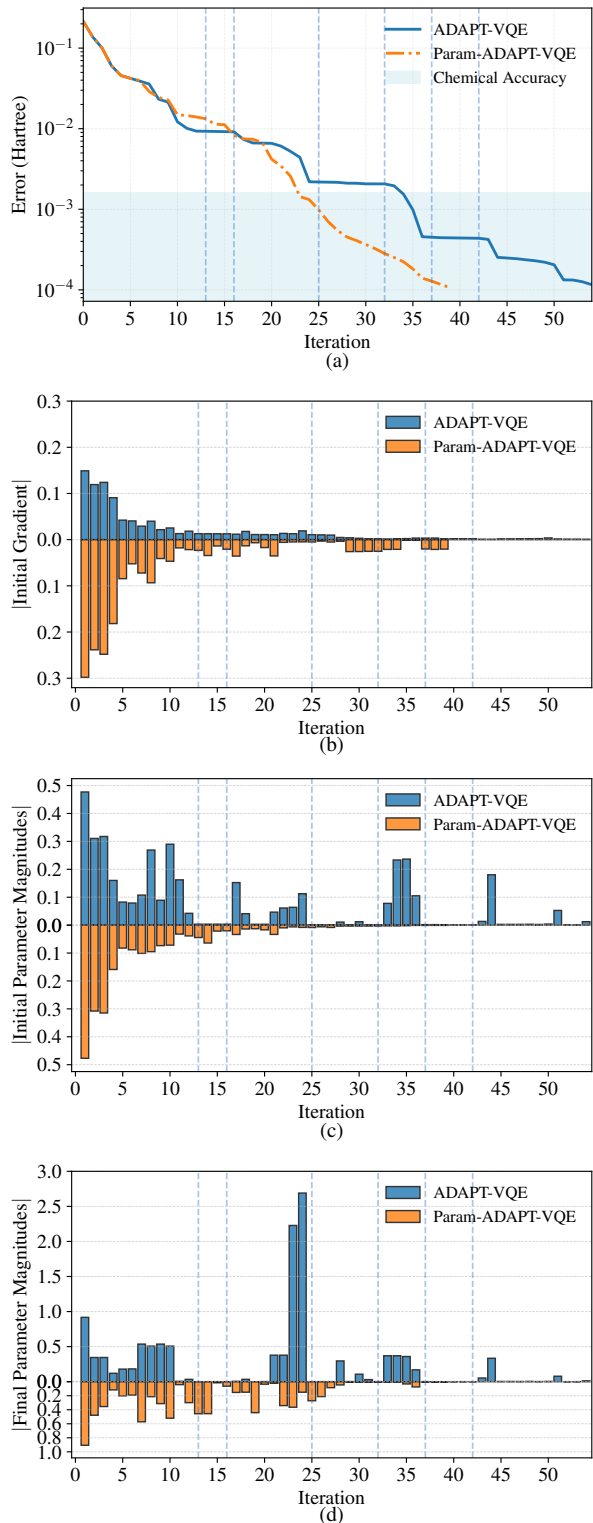


FIG. 1: Variations in (a) energy error, (b) initial gradient magnitudes of newly added operators, (c) initial parameter magnitudes of newly added operators, and (d) final parameter magnitudes of all variational parameters in the ansatz with respect to iteration number in the ground-state simulation of the BeH_2 molecule ($R(\text{Be-H})=2.6\text{\AA}$).

a 28% reduction in operator count.

Here, an excitation operator is regarded as redundant if it contributes almost no energy reduction and its parameter value nearly vanishes after optimization [23]. To identify the redundant operators involved in ansatz construction, the iterative process is partitioned into distinct regions using vertical blue dashed lines for the ADAPT-VQE results. These regions alternate between error-decreasing intervals and flat regions: the former denotes stages where the newly added excitation operators effectively induce a reduction in energy error, while the latter corresponds to periods where the total energy remains nearly constant despite continued iteration and the introduction of additional operators. Notably, ADAPT-VQE exhibits three distinct error plateaus — i.e., iteration steps from 13 to 16, 25 to 32, and 37 to 42 — demarcated by dashed lines. In contrast, Param-ADAPT-VQE achieves a consistent reduction in energy error at each iteration, with no redundant excitation operators being introduced.

Figure 1(b) shows the initial gradient magnitudes of newly added excitation operators at each iteration. ADAPT-VQE exhibits considerable gradient magnitudes across both error-decreasing intervals and flat regions; however, only negligible performance improvement is observed in the latter according to Figure 1(a). In contrast, for the iteration steps around the 25th, the excitation operators selected by Param-ADAPT-VQE exhibit smaller gradient magnitudes than those of ADAPT-VQE, yet induce a more pronounced reduction in energy error. These observations imply that operators with the largest initial gradient magnitudes do not necessarily yield effective energy reduction, and that gradient is not an infallible selection criterion.

Figure 1(c) presents the magnitudes of the parameter values of newly added excitation operators after VQE optimization at each iteration, which we refer to as the initial parameter magnitudes. It can be observed that in the error flat regions of ADAPT-VQE, excitation operators selected by the gradient-based criterion exhibit nearly zero parameter values — indicating these operators exert no significant effect and are thus redundant. In contrast, operators selected via the parameter-based criterion in Param-ADAPT-VQE exhibit notable parameter magnitudes, corresponding to more pronounced contributions to the system. This figure reveals that parameter values serve as a more reliable selection criterion than gradient magnitudes for ansatz construction.

Figure 1(d) depicts the final optimized parameter magnitudes of all variational parameters after the last iteration. It can be seen that within the flat regions, most of the parameter values for ADAPT-VQE are nearly zero, confirming these operators are redundant. In contrast, Param-ADAPT-VQE yields considerable magnitudes for most parameters, demonstrating their significant contributions to the system's total energy.

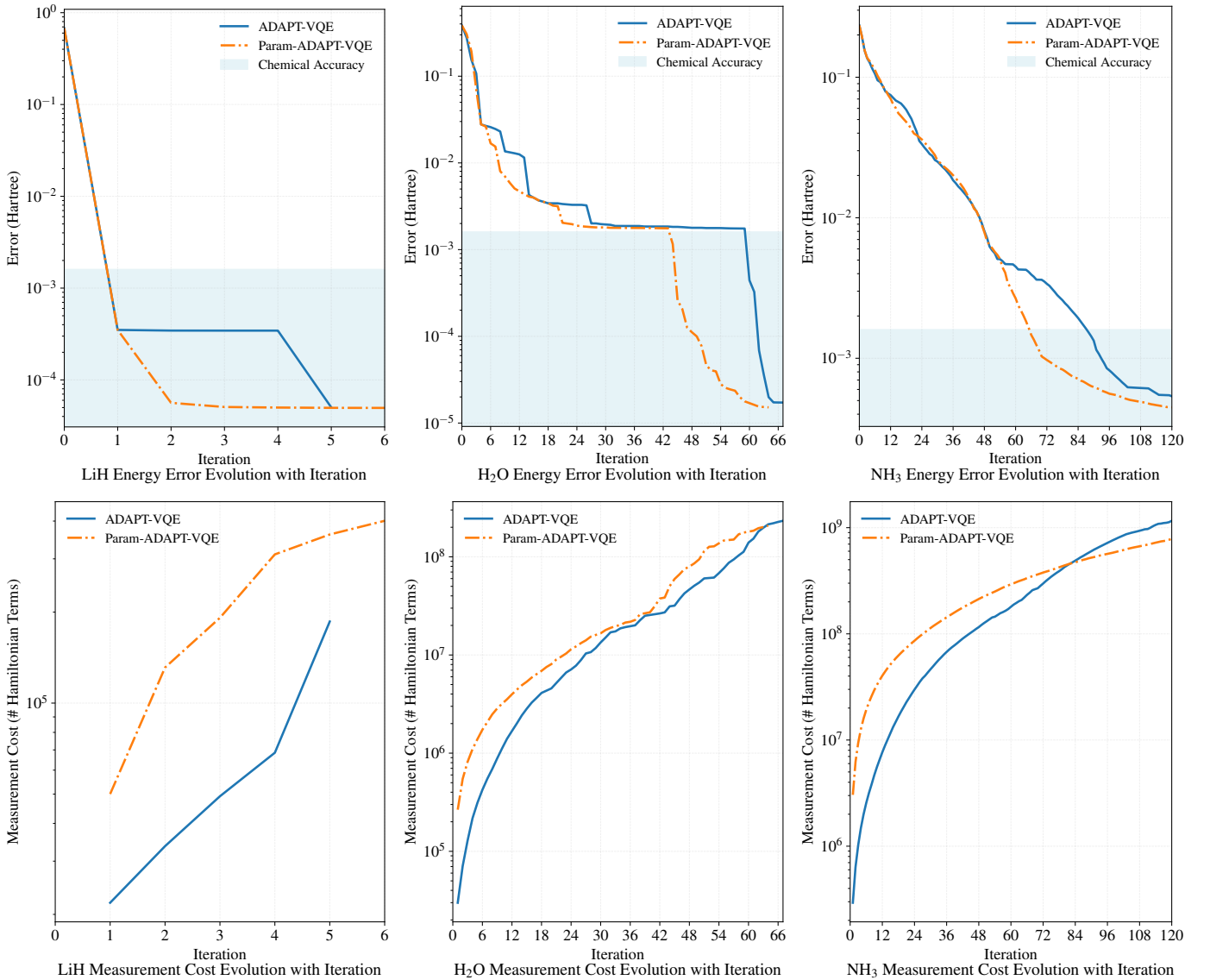


FIG. 2: (a–c) Energy error and (d–f) measurement cost as functions of iteration number on LiH, H₂O, and NH₃ with uniformly stretched bond lengths of 3.24 Å, 2.06 Å, and 1.6 Å, respectively.

B. Benchmark Studies on Extended Molecular Systems

This subsection presents systematic benchmark studies of Param-ADAPT-VQE on three prototypical molecules (LiH, H₂O, NH₃), evaluating its performance against ADAPT-VQE across three key practical metrics: energy error, parameter count, and measurement cost. To emulate strongly correlated systems, the bond lengths of these molecules are uniformly stretched, i.e., R(Li-H)=3.24 Å for LiH, R(O-H)=2.06 Å for H₂O, and R(N-H)=1.6 Å for NH₃, respectively.

Figure 2(a) - (c) depicts the evolution of energy error for the three molecules as a function of increasing iteration number (i.e., the number of excitation operators) for the two competing algorithms, respectively. Over-

all, Param-ADAPT-VQE achieves higher accuracy with fewer excitation operators compared to ADAPT-VQE.

Specifically, Figure 2(a) shows that for LiH to reach an accuracy of 10⁻⁴ Hartree, ADAPT-VQE requires 5 excitation operators while Param-ADAPT-VQE only needs 2, representing a 60.00% reduction. Figure 2(b) illustrates that for H₂O at the 10⁻⁴ Hartree accuracy, ADAPT-VQE demands 62 excitation operators versus merely 49 for Param-ADAPT-VQE, a 20.97% reduction. Figure 2(c) demonstrates that to achieve 10⁻³ Hartree accuracy, ADAPT-VQE needs 93 excitation operators whereas Param-ADAPT-VQE requires 72, corresponding to a 22.58% reduction.

Figure 2(d) - (f) presents the corresponding measurement cost as a function of iteration number for the three molecules. The measurement cost here is quantified by

the number of terms in the fermionic Hamiltonian for which expectation values need to be considered. To provide a general reference, the simultaneous measurement [40] and measurement reuse [41] techniques are not considered in this work. We observe that the measurement cost of Param-ADAPT-VQE rises at a faster rate in the initial stage, owing to the additional local VQE optimization performed on all excitation operators in the pool during its operator selection process. However, as iterations proceed, the variational parameters in the ansatz accumulate progressively, and the measurement cost required for each global optimization step increases substantially, ultimately surpassing that of the local VQE optimization.

Specifically, Figure 2(a) and (d) shows that for LiH at an energy error of 10^{-4} Hartree, the measurement cost of ADAPT-VQE reaches 1.86×10^6 , while that of Param-ADAPT-VQE is only 1.31×10^6 , representing a 29.55% reduction. Figure 2(b) and (e) reveals that for H₂O at the same 10^{-4} Hartree accuracy, the measurement cost of ADAPT-VQE reaches 1.81×10^9 , while that of Param-ADAPT-VQE is only 8.57×10^8 , corresponding to a 52.62% reduction. Figure 2(c) and (f) demonstrates that for NH₃ at an energy error of 10^{-3} Hartree, the measurement cost of ADAPT-VQE reaches 6.59×10^9 , while that of Param-ADAPT-VQE is only 3.78×10^9 , a 42.67% reduction. A key insight emerging from these results is that Param-ADAPT-VQE surpasses ADAPT-VQE in both accuracy and quantum measurement cost for all systems after the 81st iteration.

In addition, performance comparisons between Param-ADAPT-VQE and ADAPT-VQE across an expanded set of molecules (H₄, LiH, HF, BeH₂, H₂O, and NH₃ at varying bond lengths) are provided in the Appendix for reference. The key conclusions drawn from these extended analyses are generally consistent with the aforementioned findings.

The above results demonstrate that within the ADAPT-VQE framework, the parameter-based criterion for excitation operator selection effectively reduces the redundancy rate in the ansatz compared with the gradient-based criterion. Furthermore, the adoption of sub-Hamiltonian and hot-start yields a further reduction in quantum measurement cost relative to warm-start. In summary, Param-ADAPT-VQE exhibits distinct advantages over ADAPT-VQE with respect to both ansatz depth and measurement cost.

IV. CONCLUSION

In this work, we propose the Param-ADAPT-VQE, a novel algorithm for selecting excitation operators via

a parameter-based criterion. We characterize the features of redundant operators through concrete case studies and demonstrate that Param-ADAPT-VQE can effectively reduce the proportion of redundant operators in the ansatz. A sub-Hamiltonian technique is devised to avoid the significant increase in measurement cost incurred by operator pool scanning. Furthermore, we adopt a hot-start optimization strategy, which cut down the measurement cost associated with global VQE optimization by place the global VQE optimization to a start point closer to the optimal solution, therefore reduces the number of optimization iterations. Numerical implementations on molecular systems including LiH, H₂O and NH₃ show that the Param-ADAPT-VQE outperforms ADAPT-VQE in terms of the number of excitation operators, computational accuracy, and measurement cost metrics. Moreover, our algorithm is fully compatible with modified versions of ADAPT-VQE, thus allowing further specific performance gains.

DATA AVAILABILITY

All data were generated with the code publicly available at https://atomgit.com/mindspore/mindquantum/tree/research/paper_with_code/Param_ADAPT_VQE.

CODE AVAILABILITY

The code used for the numerical simulations has been made publicly available at https://atomgit.com/mindspore/mindquantum/tree/research/paper_with_code/Param_ADAPT_VQE.

ACKNOWLEDGEMENTS

This work was supported by the Innovation Program for Quantum Science and Technology under Grant No. 2024ZD0300502, and the Beijing Nova Program under Grant No. 20240484652.

Appendix A

To further validate the robustness of our findings, this appendix presents a comprehensive performance comparison between Param-ADAPT-VQE and ADAPT-VQE for H₄ (Figure 3), LiH (Figure 4), HF (Figure 5), H₂O (Figure 6), BeH₂ (Figure 7) and NH₃ (Figure 8) across a range of bond lengths. The key conclusions drawn from these supplementary analyses are generally consistent with the core results reported in the main text.

[1] A. Szabo and N. S. Ostlund, *Modern quantum chemistry: introduction to advanced electronic structure theories* (Courier Corporation, 1996).

ory (Courier Corporation, 1996).

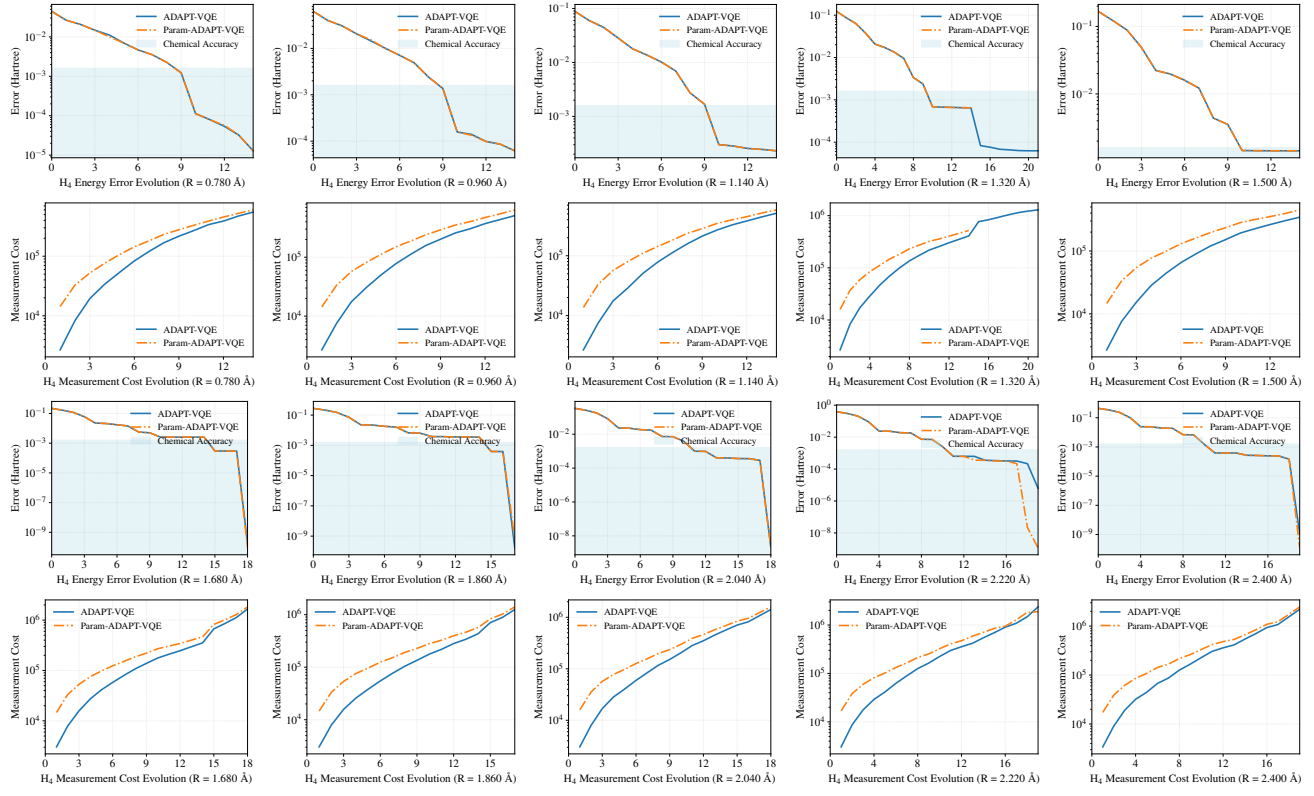


FIG. 3: Evolution of energy error and measurement cost with iteration for H_4 at different bond lengths.

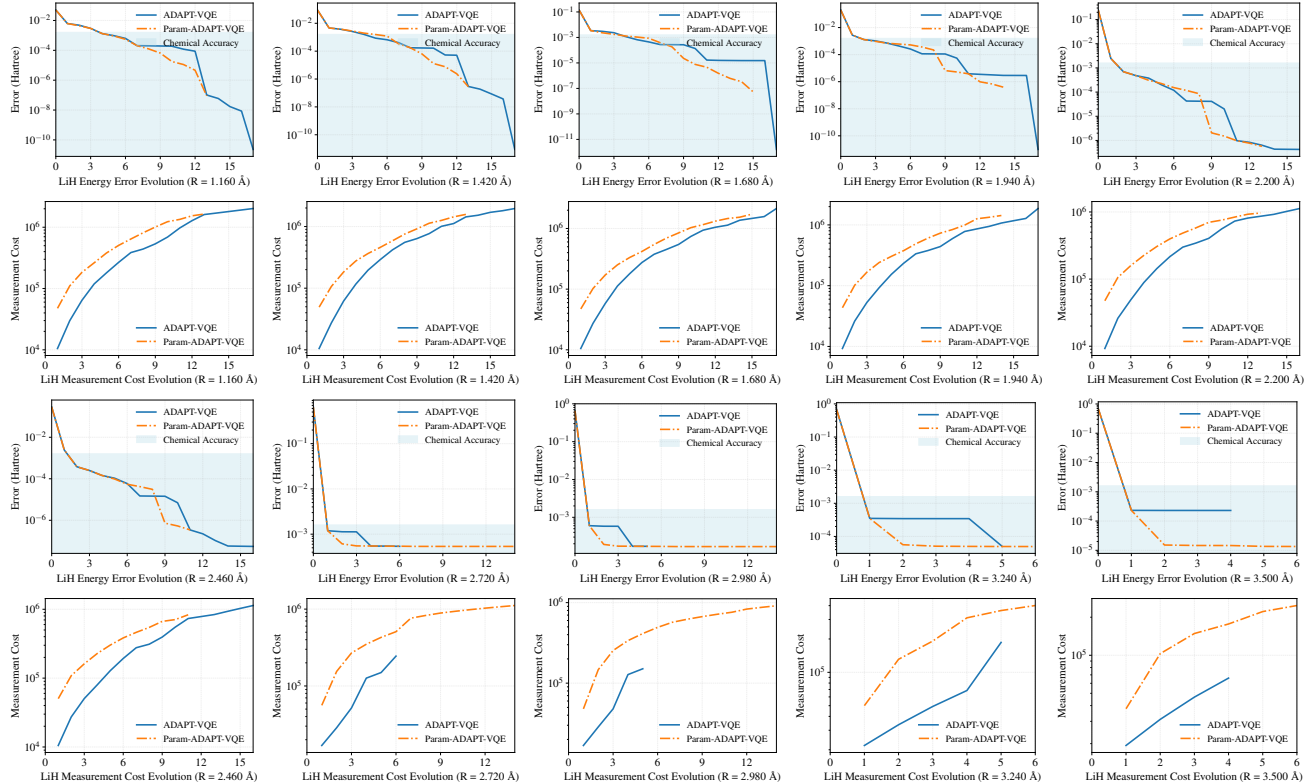


FIG. 4: Evolution of energy error and measurement cost with iteration for LiH at different bond lengths.

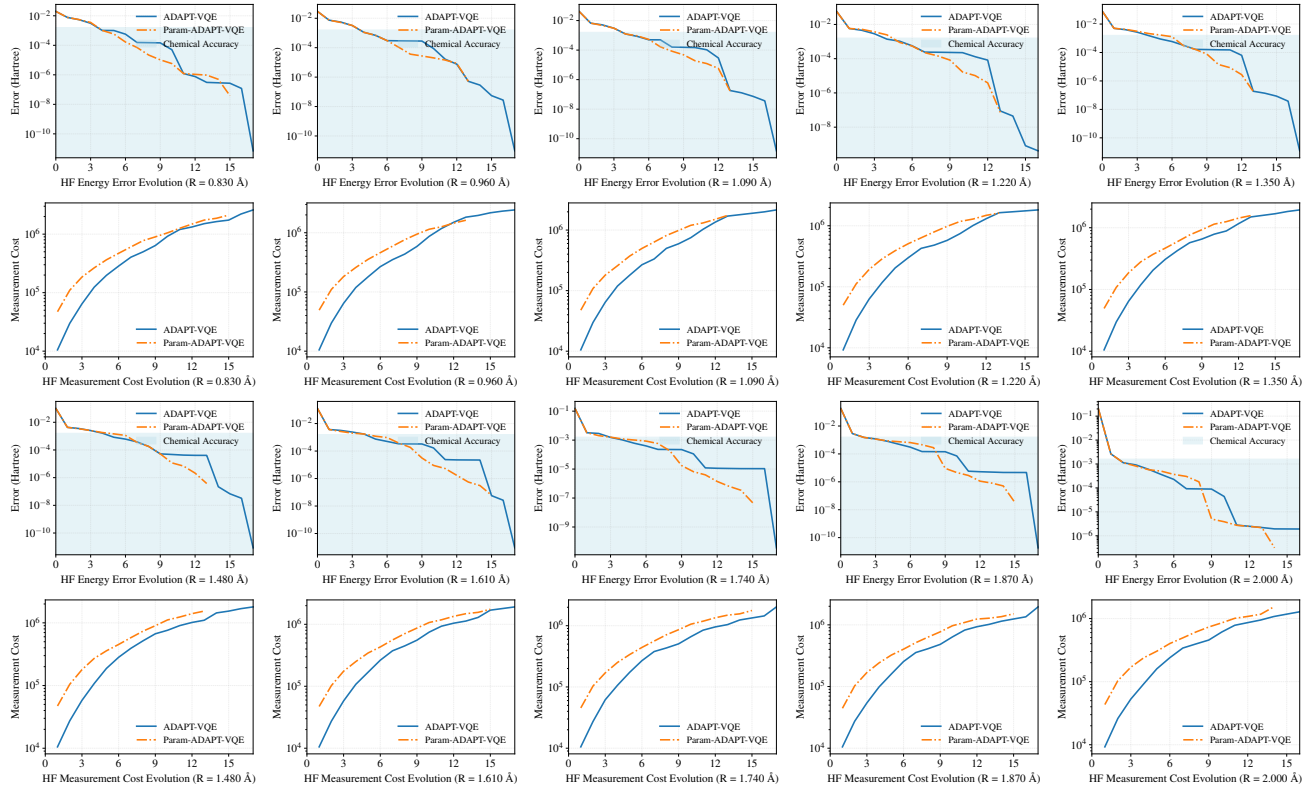


FIG. 5: Evolution of energy error and measurement cost with iteration for HF at different bond lengths.

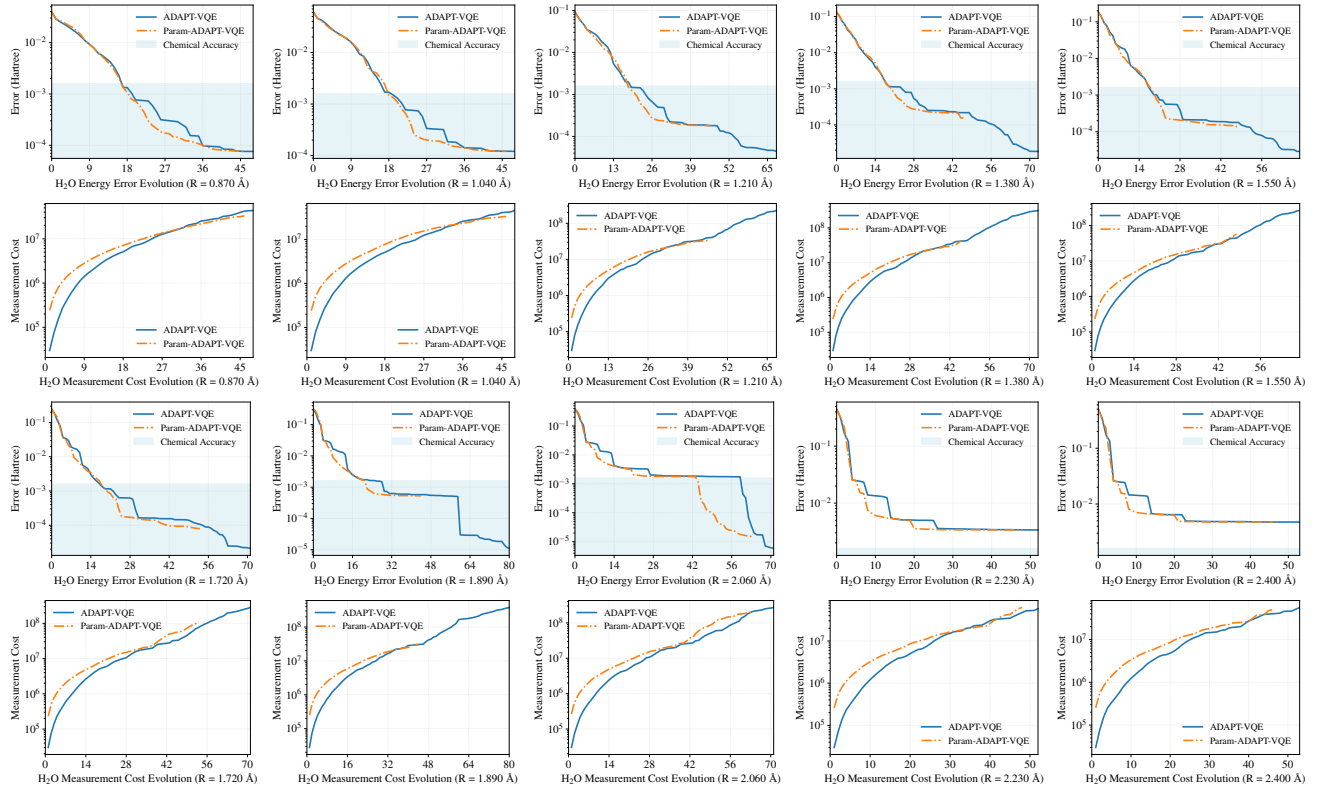
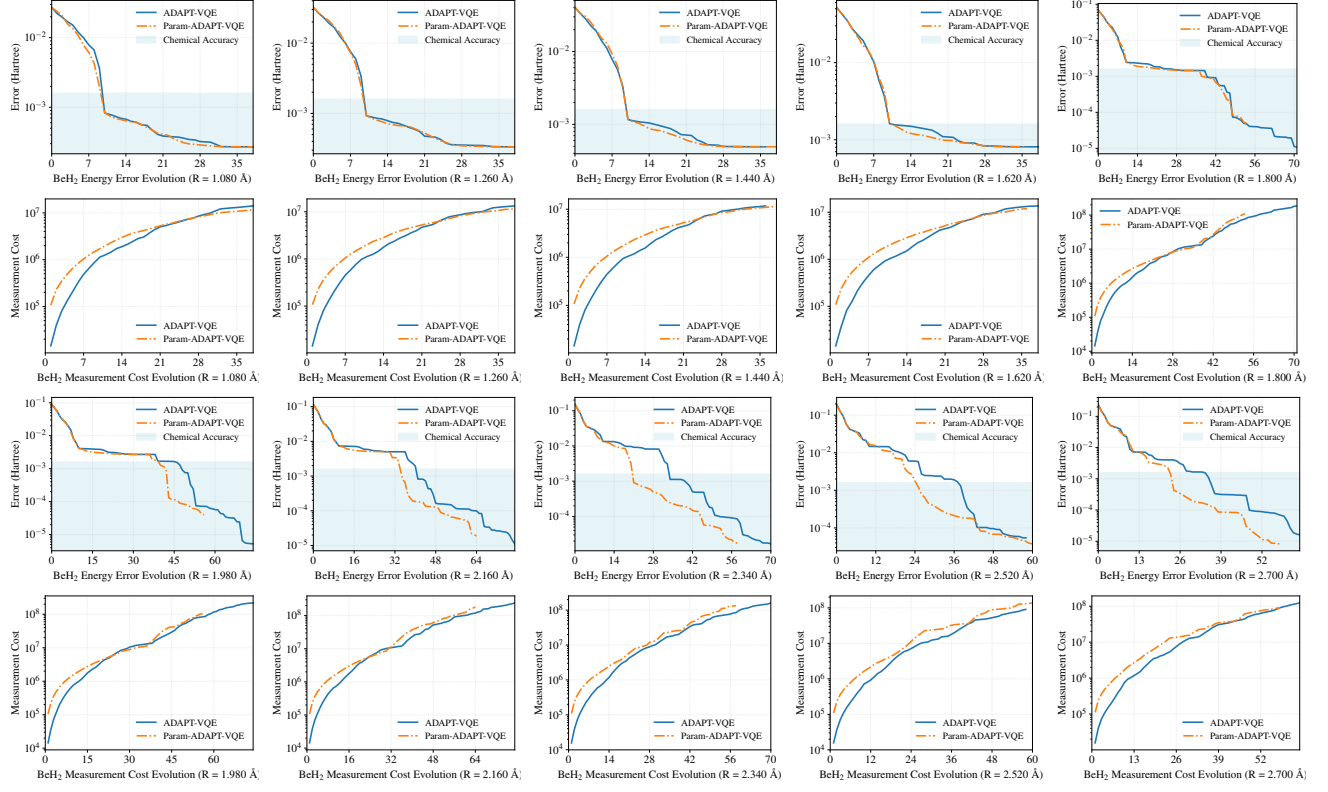
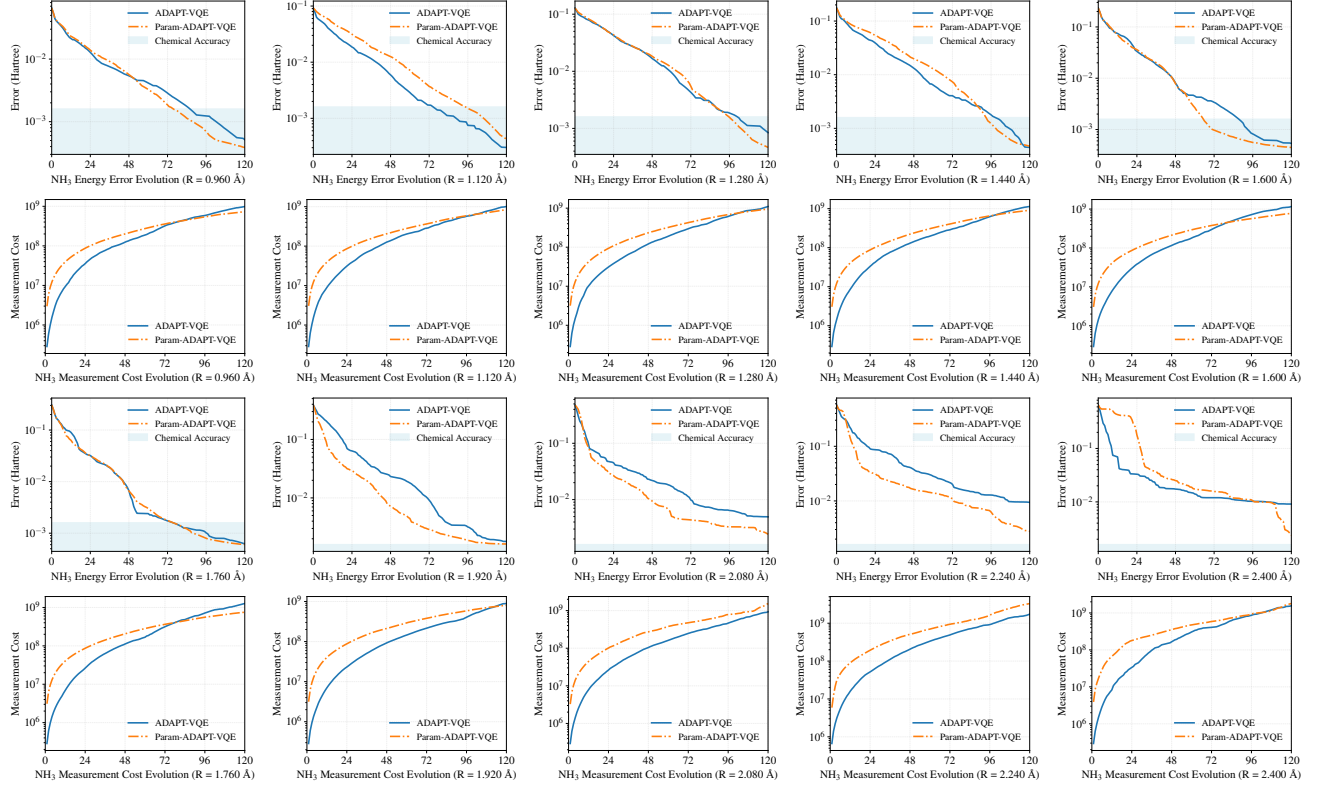


FIG. 6: Evolution of energy error and measurement cost with iteration for H₂O at different bond lengths.

FIG. 7: Evolution of energy error and measurement cost with iteration for BeH_2 at different bond lengths.FIG. 8: Evolution of energy error and measurement cost with iteration for NH_3 at different bond lengths.

[2] T. Helgaker, S. Coriani, P. Jørgensen, K. Kristensen, J. Olsen, and K. Ruud, Recent advances in wave function-based methods of molecular-property calculations, *Chemical reviews* **112**, 543 (2012).

[3] S. McArdle, S. Endo, A. Aspuru-Guzik, S. C. Benjamin, and X. Yuan, Quantum computational chemistry, *Reviews of Modern Physics* **92**, 015003 (2020).

[4] M. A. Nielsen and I. L. Chuang, *Quantum Computation and Quantum Information 10th Anniversary Edition* (Cambridge University Press, 2010).

[5] A. Peruzzo, J. McClean, P. Shadbolt, M.-H. Yung, X.-Q. Zhou, P. J. Love, A. Aspuru-Guzik, and J. L. O'brien, A variational eigenvalue solver on a photonic quantum processor, *Nature communications* **5**, 4213 (2014).

[6] J. Tilly, H. Chen, S. Cao, D. Picozzi, K. Setia, Y. Li, E. Grant, L. Wossnig, I. Rungger, G. H. Booth, *et al.*, The variational quantum eigensolver: a review of methods and best practices, *Physics Reports* **986**, 1 (2022).

[7] M. Cerezo, A. Arrasmith, R. Babbush, S. C. Benjamin, S. Endo, K. Fujii, J. R. McClean, K. Mitarai, X. Yuan, L. Cincio, *et al.*, Variational quantum algorithms, *Nature Reviews Physics* **3**, 625 (2021).

[8] S. H. Gould, *Variational methods for eigenvalue problems: an introduction to the Weinstein method of intermediate problems* (University of Toronto Press, 1966).

[9] J. Preskill, Quantum computing in the nisq era and beyond, *Quantum* **2**, 79 (2018).

[10] J. Romero, R. Babbush, J. R. McClean, C. Hempel, P. J. Love, and A. Aspuru-Guzik, Strategies for quantum computing molecular energies using the unitary coupled cluster ansatz, *Quantum Science and Technology* **4**, 014008 (2018).

[11] C. Cao, J. Hu, W. Zhang, X. Xu, D. Chen, F. Yu, J. Li, H.-S. Hu, D. Lv, and M.-H. Yung, Progress toward larger molecular simulation on a quantum computer: Simulating a system with up to 28 qubits accelerated by point-group symmetry, *Physical Review A* **105**, 062452 (2022).

[12] R. He, A. Abilimit, X. Hong, Q. Chai, J. Zhou, J. Guan, G. Cui, and S. Ying, Hamiltonian-informed point group symmetry-respecting ansatz for variational quantum eigensolver, *arXiv preprint arXiv:2512.21087* (2025).

[13] H. R. Grimsley, S. E. Economou, E. Barnes, and N. J. Mayhall, An adaptive variational algorithm for exact molecular simulations on a quantum computer, *Nature communications* **10**, 3007 (2019).

[14] J. R. McClean, S. Boixo, V. N. Smelyanskiy, R. Babbush, and H. Neven, Barren plateaus in quantum neural network training landscapes, *Nature communications* **9**, 4812 (2018).

[15] H. R. Grimsley, G. S. Barron, E. Barnes, S. E. Economou, and N. J. Mayhall, Adaptive, problem-tailored variational quantum eigensolver mitigates rough parameter landscapes and barren plateaus, *npj Quantum Information* **9**, 19 (2023).

[16] P. G. Anastasiou, Y. Chen, N. J. Mayhall, E. Barnes, and S. E. Economou, Tetris-adapt-vqe: An adaptive algorithm that yields shallower, denser circuit ansätze, *Physical Review Research* **6**, 013254 (2024).

[17] Z. Lan and W. Liang, Amplitude reordering accelerates the adaptive variational quantum eigensolver algorithms, *Journal of Chemical Theory and Computation* **18**, 5267 (2022).

[18] V. O. Shkolnikov, N. J. Mayhall, S. E. Economou, and E. Barnes, Avoiding symmetry roadblocks and minimiz-
ing the measurement overhead of adaptive variational quantum eigensolvers, *Quantum* **7**, 1040 (2023).

[19] L. W. Bertels, H. R. Grimsley, S. E. Economou, E. Barnes, and N. J. Mayhall, Symmetry breaking slows convergence of the adapt variational quantum eigensolver, *Journal of Chemical Theory and Computation* **18**, 6656 (2022).

[20] M. Ramôa, P. G. Anastasiou, L. P. Santos, N. J. Mayhall, E. Barnes, and S. E. Economou, Reducing the resources required by adapt-vqe using coupled exchange operators and improved subroutines, *npj Quantum Information* **11**, 86 (2025).

[21] Y. Fan, C. Cao, X. Xu, Z. Li, D. Lv, and M.-H. Yung, Circuit-depth reduction of unitary-coupled-cluster ansatz by energy sorting, *The Journal of Physical Chemistry Letters* **14**, 9596 (2023).

[22] V. O. Shkolnikov, N. J. Mayhall, S. E. Economou, and E. Barnes, Avoiding symmetry roadblocks and minimizing the measurement overhead of adaptive variational quantum eigensolvers, *Quantum* **7**, 1040 (2023).

[23] N. Vaquero-Sabater, A. Carreras, and D. Casanova, Pruned-adapt-vqe: compacting molecular ansatze by removing irrelevant operators, *Journal of Chemical Theory and Computation* **21**, 8720 (2025).

[24] Y. S. Yordanov, V. Armaos, C. H. Barnes, and D. R. Arvidsson-Shukur, Qubit-excitation-based adaptive variational quantum eigensolver, *Communications Physics* **4**, 228 (2021).

[25] H. L. Tang, V. Shkolnikov, G. S. Barron, H. R. Grimsley, N. J. Mayhall, E. Barnes, and S. E. Economou, qubit-adapt-vqe: An adaptive algorithm for constructing hardware-efficient ansatze on a quantum processor, *PRX Quantum* **2**, 020310 (2021).

[26] J. Liu, Z. Li, and J. Yang, An efficient adaptive variational quantum solver of the schrödinger equation based on reduced density matrices, *The Journal of chemical physics* **154** (2021).

[27] P. Jordan and E. P. Wigner, *Über das paulische äquivalenzverbot* (Springer, 1993).

[28] N. Hatano and M. Suzuki, Finding exponential product formulas of higher orders, in *Quantum annealing and other optimization methods* (Springer, 2005) pp. 37–68.

[29] P. K. Barkoutsos, J. F. Gonthier, I. Sokolov, N. Moll, G. Salis, A. Fuhrer, M. Ganzhorn, D. J. Egger, M. Troyer, A. Mezzacapo, *et al.*, Quantum algorithms for electronic structure calculations: Particle-hole hamiltonian and optimized wave-function expansions, *Physical Review A* **98**, 022322 (2018).

[30] G. Li, A. Wu, Y. Shi, A. Javadi-Abhari, Y. Ding, and Y. Xie, Paulihedral: a generalized block-wise compiler optimization framework for quantum simulation kernels, in *Proceedings of the 27th ACM International Conference on Architectural Support for Programming Languages and Operating Systems* (2022) pp. 554–569.

[31] Z. He, D. Zgid, A. Kemper, and J. Freericks, Classical reservoir approach for efficient molecular ground state preparation, *arXiv preprint arXiv:2512.21069* (2025).

[32] Z. Sun, X. Li, J. Liu, Z. Li, and J. Yang, Circuit-efficient qubit excitation-based variational quantum eigensolver, *Journal of Chemical Theory and Computation* (2025).

[33] Y. S. Yordanov, D. R. Arvidsson-Shukur, and C. H. Barnes, Efficient quantum circuits for quantum computational chemistry, *Physical Review A* **102**, 062612 (2020).

[34] M. Schuld, V. Bergholm, C. Gogolin, J. Izaac, and N. Killoran, Evaluating analytic gradients on quantum hardware, *Physical Review A* **99**, 032331 (2019).

[35] R. Sweke, F. Wilde, J. Meyer, M. Schuld, P. K. Fährmann, B. Meynard-Piganeau, and J. Eisert, Stochastic gradient descent for hybrid quantum-classical optimization, *Quantum* **4**, 314 (2020).

[36] C. G. Broyden, Quasi-newton methods and their application to function minimisation, *Mathematics of Computation* **21**, 368 (1967).

[37] Q. Sun, T. C. Berkelbach, N. S. Blunt, G. H. Booth, S. Guo, Z. Li, J. Liu, J. D. McClain, E. R. Sayfutyarova, S. Sharma, *et al.*, Pyscf: the python-based simulations of chemistry framework, *Wiley Interdisciplinary Reviews: Computational Molecular Science* **8**, e1340 (2018).

[38] X. Xu, J. Cui, Z. Cui, R. He, Q. Li, X. Li, Y. Lin, J. Liu, W. Liu, J. Lu, M. Luo, C. Lyu, S. Pan, M. Pavel, R. Shu, J. Tang, R. Xu, S. Xu, K. Yang, F. Yu, Q. Zeng, H. Zhao, Q. Zheng, J. Zhou, X. Zhou, Y. Zhu, Z. Zou, A. Bayat, X. Cao, W. Cui, Z. Li, G. Long, Z. Su, X. Wang, Z. Wang, S. Wei, R.-B. Wu, P. Zhang, and M.-H. Yung, Mindspore quantum: A user-friendly, high-performance, and ai-compatible quantum computing framework (2024), arXiv:2406.17248 [quant-ph].

[39] P. Virtanen, R. Gommers, T. E. Oliphant, M. Haberland, T. Reddy, D. Cournapeau, E. Burovski, P. Peterson, W. Weckesser, J. Bright, *et al.*, Scipy 1.0: fundamental algorithms for scientific computing in python, *Nature methods* **17**, 261 (2020).

[40] P. Gokhale, O. Angiuli, Y. Ding, K. Gui, T. Tomesh, M. Suchara, M. Martonosi, and F. T. Chong, $o(n^3)$ measurement cost for variational quantum eigensolver on molecular hamiltonians, *IEEE Transactions on Quantum Engineering* **1**, 1 (2020).

[41] A. Ikhtiarudin, G. K. Sunnardianto, F. Fathurrahman, M. K. Agusta, and H. K. Diponjono, Shot-efficient adapt-vqe via reused pauli measurements and variance-based shot allocation, arXiv preprint arXiv:2507.16879 (2025).